Phantom Matter: A Challenging Solution to the Cosmological Tensions

Adrià Gómez-Valent and Joan Solà Peracaula
Departament de Física Quàntica i Astrofísica and Institute of Cosmos Sciences, Universitat de Barcelona, Av. Diagonal 647, E-08028 Barcelona, Catalonia, Spain

Abstract

The idea of composite dark energy (DE) is quite natural since on general grounds we expect that the vacuum energy density (associated with the cosmological term Λ) may appear in combination with other effective forms of DE, denoted X. Here we deal with model wXCDM, a simplified version of the old ΛXCDM model, and exploit the possibility that X behaves as "phantom matter" (PM), which appears in stringy versions of the running vacuum model (RVM). Unlike phantom DE, the PM fluid satisfies the strong energy condition like usual matter, hence bringing to bear positive pressure at the expense of negative energy. Bubbles of PM may appear in the manner of a transitory "phantom vacuum" tunneled into the late Universe before it heads toward a new de Sitter era, thereby offering a crop field for the growing of structures earlier than expected. Using Type Ia supernovae, cosmic chronometers, transversal baryon acoustic oscillations (BAO 2D), large-scale structure data, and the full cosmic microwave background likelihood from Planck 2018, we find that the H_0 and growth tensions virtually disappear, provided that BAO 2D are the only source of BAO data used in the fit. In contrast, our preliminary analysis using exclusively anisotropic BAO (BAO 3D) indicates that the ability to ease the H_0 tension is significantly reduced as compared to the scenario with BAO 2D, despite the fact that the overall fit to the cosmological data is still better than in the ΛCDM. Finally, our approach with BAO 2D favors quintessence-like behavior of the DE below $z \simeq 1.5$ at $\gtrsim 3\sigma$ confidence level, which is compatible with the recent DESI measurements.

Unified Astronomy Thesaurus concepts: Cosmology (343); Cosmological models (337); Cosmological parameters (339); Cosmological evolution (336); Dark energy (351); Large-scale structure of the universe (902)

1. Introduction

The standard (or concordance) cosmological model, aka ΛCDM, has been a rather successful paradigm for the description of the Universe for more than three decades (P. J. E. Peebles 1993), especially since the late 1990s (M. S. Turner 2022). Despite that it constitutes the main theoretical pillar at our hands for the description of the Universe's evolution within the general relativity context, the ΛCDM is being pestered by a number of glitches and hitches that prove to be more and more difficult to iron out. While the model is presumably right in the main (at least at a pure phenomenological level), an increasing number of worrisome inconsistencies (or "tensions") have been perturbing its reputation and its future prospects. For a long time the role played by a rigid cosmological constant (CC) Λ in the standard ΛCDM model has been rather successful since it has provided a fairly reasonable description of the overall cosmological data (P. A. R. Ade et al. 2016; N. Aghanim et al. 2020). But the use of the cosmological term has never been fully clarified at the formal theoretical level since it is usually associated with the so-called "cosmological constant problem," a serious conundrum that has been amply discussed in the literature (see e.g., S. Weinberg 1989; T. Padmanabhan 2003; P. J. E. Peebles & B. Ratra 2003; J. Solà 2013; J. Solà Peracaula 2022, and references therein). Inasmuch as the vacuum energy density (VED) is related to Λ through $\rho_{\rm vac} = \Lambda/(8\pi G_{\rm N})$ ($G_{\rm N}$ being Newton's gravitational coupling), the conceptual fate of Λ is tied to our ultimate understanding of the VED on fundamental physical terms. Fortunately, recent theoretical developments on the VED in quantum field theory (QFT) are bringing new light for a potential alleviation of these theoretical difficulties. In fact, the possibility that the quantum vacuum (and hence that Λ itself) is actually dynamical (i.e., evolving with the cosmological expansion) rather than being stuck at a rigid value has lately been substantiated in the context of QFT in curved spacetime (J. Solà 2013; J. Solà Peracaula 2022), as well as in the framework of low-energy effective string theory (N. E. Mavromatos & J. Solà Peracaula 2021b, 2021a) and, very recently, in lattice quantum gravity (M. Dai et al. 2024). For a long time, the dynamics of the VED has been popularly addressed on phenomenological grounds using ad hoc scalar fields (quintessence and the like) that supplant the role of the Λ-term through the current value of some suitable effective potential (T. Padmanabhan 2003; P. J. E. Peebles & B. Ratra 2003; see e.g., O. Avsajanishvili et al. 2024, for a recent review). Currently, the first data release of the Dark Energy Spectroscopic Instrument (DESI) suggests tantalizing evidence that the dark energy (DE) might be dynamical using some common parameterizations of the DE (A. G. Adame et al. 2024). More detailed analyses will be needed before getting a final confirmation, of course, but it is a fact that some anticipatory (and fairly robust) hints of dynamical DE in the literature already pointed out this possibility a few years ago from different perspectives and using a significant amount of cosmological data. The level of evidence put forward by these anticipatory studies was substantial and ranged from 3σ to 4σ. Some of these analyses are well-known (J. Solà et al. 2015, 2017; J. Solà Peracaula et al. 2017, 2018a, 2018b; A. Gómez-Valent & J. Solà Peracaula 2018) and involved the running vacuum model (RVM).[1] Subsequent analysis around

---

[1] For a review, see, e.g., J. Solà (2013), J. Solà & A. Gòmez-Valent (2015), and J. Solà Peracaula (2022) and references therein.

the same time also supported this possibility using different methods and parameterizations (G.-B. Zhao et al. 2017; J. Solà Peracaula et al. 2019).

Dynamical DE could also impinge positively on the resolution of the cosmological tensions. Let us recall that these are mainly concerned with the measurement of the current Hubble parameter $H_0 \equiv 100h \, \mathrm{km \, s^{-1} \, Mpc}$ and the growth of large-scale structures (LSSs). The latter is usually monitored with S_8 or σ_8, or even better using a parameter σ_{12} defining the amplitude of the matter power spectrum at fixed spheres of radius 12 Mpc rather than $8 \, h^{-1}$ Mpc, thus avoiding artificial dependence on the value of h (A. G. Sanchez 2020; A. Semenaite et al. 2022, 2023).[2] The first kind of tension involves a serious disagreement between the cosmic microwave background (CMB) observations, using fiducial ΛCDM cosmology, and the local direct (distance ladder) measurements of the Hubble parameter today. It is arguably the most puzzling open question, and it leads to a severe inconsistency of $\sim 5\sigma$ confidence level (CL) between the mentioned observables. The second kind of tension is related to the exceeding rate of LSS formation in the late Universe predicted by the ΛCDM as compared to measurements, although the discordance here is moderate, at a CL of $\sim 2\sigma{-}3\sigma$. More recently, data from the James Webb Space Telescope (JWST; J. P. Gardner et al. 2006; I. Labbé et al. 2023) have revealed the existence of an unexpectedly large population of extremely massive galaxies at large redshifts $z \gtrsim 5{-}10$, a fact that is also strongly at odds with the prospects of the concordance model.

There is a wide panoply of strategies in the literature trying to mitigate some of the above tensions, although at present we may be still far away from a satisfactory resolution of the situation. We mention only a few. It has been argued that within the class of models where the DE is dealt with as a cosmic fluid with equation of state (EOS) $w(z)$, solving the H_0 tension demands the phantom condition $w(z) < -1$ at some z, whereas solving both the H_0 and σ_8 tensions requires $w(z)$ to cross the phantom divide and/or other sorts of exotic transitions (see, e.g., G. Alestas et al. 2021, 2022; V. Marra & L. Perivolaropoulos 2021; L. Perivolaropoulos & F. Skara 2021, 2022b; L. Heisenberg et al. 2022; A. Gomez-Valent et al. 2024). The possibility of a sign flip of the Λ term has been entertained in recent times, e.g., in R. Calderón et al. (2021). Let us also mention the model analyzed in Ö. Akarsu et al. (2021, 2023) (based on the framework of Ö. Akarsu et al. 2020), in which one considers a sudden transition from the anti −de Sitter (AdS; $\Lambda < 0$) to de Sitter (dS) regime ($\Lambda > 0$) occurring near our time. Despite it being essentially ad hoc, the model yields a rather good fit to the data when transversal/angular baryon acoustic oscillations (BAO; BAO 2D for short) is employed in the fitting analysis (see also A. Gomez-Valent et al. 2024). Actually, a more general framework already existed long ago, namely the ΛXCDM model (J. Grande et al. 2006, 2007, 2009), where the running vacuum and an extra X component can exchange energy. In such a context, one can have $\Lambda < 0$ or $\Lambda > 0$.

In this work, we further exploit the virtues of the ΛXCDM, which is an enhanced family of RVMs (J. Solà Peracaula 2022). The linchpin of the RVM framework is the dynamical nature of the VED framed in the fundamental context of QFT in curved spacetime or in low-energy string theory. Appropriate renormalization in this context gets rid of the quartic mass terms $\sim m^4$ responsible for the fine-tuning troubles, and as a result, the VED becomes a smooth function of even powers of the Hubble rate (C. Moreno-Pulido & J. Solà 2020; C. Moreno-Pulido & J. Solà Peracaula 2022a, 2022b; C. Moreno-Pulido et al. 2023). This leads to a fairly good description of the cosmological data and helps ease the tensions (J. Solà Peracaula et al. 2021, 2023). Worth noticing is also the phenomenological performance of the stringy version of the RVM (A. Gómez-Valent et al. 2023). That said, we cannot exclude that the DE may be a composite fluid, a possibility that could further help in the task of alleviating these tensions. For this reason a good candidate is the aforementioned "ΛXCDM model" (J. Grande et al. 2006, 2007, 2009), an RVM-born model that was initially motivated as a possible cure for the cosmic coincidence problem. In it, we have two DE components: one is the running VED, $\rho_{\mathrm{vac}} = \rho_{\mathrm{vac}}(H)$, and the other is the mentioned X. As a matter of fact, the entity X need not be a fundamental field, as emphasized in J. Grande et al. (2006); it may just be due to particular terms in the effective action that mimic a dynamical DE component. In this sense, X can have phantom-like behavior without causing an uproar at the theoretical level. Not only this, but X may even display "phantom matter" (PM) behavior (J. Grande et al. 2006), namely, an intriguing form of DE that, in stark contrast to the usual phantom DE, is characterized by a positive pressure ($p_X > 0$) at the expense of a negative energy density ($\rho_X < 0$). It is remarkable that there exists specific theoretical scenarios in the current literature that support the ΛXCDM structure with a PM-like component X. An example appears in the stringy RVM context (N. E. Mavromatos & J. Solà Peracaula 2021b, 2021a). No less remarkable is the fact that the phenomenological performance attained by such a peculiar composite DE scenario may surpass by far that of the standard ΛCDM under appropriate conditions, as we shall shortly clarify. However, for the sake of simplicity, in this paper we shall address a reduced version of the ΛXCDM, which we call the wXCDM model (not to be confused with the conventional wCDM parameterization), in which the additional X component of the ΛXCDM is kept intact, but on the other hand we mimic the running Λ with another dynamical component, which we call Y. While the analysis within the full ΛXCDM will be presented elsewhere, we shall nonetheless demonstrate here that even the simplified wXCDM model can be very efficient in dealing with the cosmological tensions. However, for this to be so, the following two conditions must be met in our analysis: (i) the X component must have the ability to behave as PM, and (ii) BAO 2D must be the only source of BAO data used in our global fit. The precise reasons for considering only this type of BAO data in the current work will be explained below, together with a preliminary discussion of the results obtained with the BAO 3D variant. The upshot is that by accepting these reasons for using BAO 2D only and also taking advantage of the mentioned (stringy) theoretical framework to accommodate PM, the possibility to quell the cosmological tensions on fundamental grounds is viable and can be extremely effective.

2. Composite Dark Energy

We next mention three related types of composite models of the DE: (i) ΛXCDM, (ii) wXCDM, and (iii) Λ_sCDM. As noted,

---

[2] See E. Di Valentino et al. (2021a, 2021b) for summarized explanations about each of these tensions and E. Abdalla et al. (2022) and L. Perivolaropoulos & F. Skara (2022a) for comprehensive reviews.

model (i) has existed in different versions since long ago (J. Grande et al. 2006, 2007, 2009). Model (ii) will be analyzed here for the first time; it constitutes a simplified version of model (i) and embodies the PM feature. Finally, model (iii) was recently analyzed in Ö. Akarsu et al. (2023).

i. ΛXCDM model. Its definition and comprehensive discussion, including the background cosmological solution, are provided in utmost detail in J. Grande et al. (2006). In addition, in J. Grande et al. (2009) the corresponding cosmic perturbation equations are fully accounted for. Here we just present a very short qualitative description. Within the ΛXCDM, the cosmic fluid contains the usual matter energy density ρ_m and a composite DE sector made out of two components: one is the running VED $\rho_{\rm vac}$, and the other is called X, with energy density ρ_X. The VED here is treated within the QFT framework of the RVM (C. Moreno-Pulido & J. Solà 2020; C. Moreno-Pulido & J. Solà Peracaula 2022a; 2022b; C. Moreno-Pulido et al. 2023), in which $\rho_{\rm vac} = \rho_{\rm vac}(H)$ evolves with the expansion rate. In the current Universe, such an evolution reads as (J. Solà Peracaula 2022)

$$\rho_{\rm vac}(H) = \rho_{\rm vac}^0 + \frac{3\nu_{\rm eff}}{8\pi}(H^2 - H_0^2)m_{\rm Pl}^2, \qquad (1)$$

with $\rho_{\rm vac}^0$ the current VED value, $m_{\rm Pl}$ the Planck mass, and $|\nu_{\rm eff}| \ll 1$ a small parameter that is formally computable in QFT; see the aforementioned papers. For $\nu_{\rm eff} > 0$ the VED decreases with the expansion and hence the RVM mimics quintessence, whereas for $\nu_{\rm eff} < 0$ the VED increases with the expansion and the RVM behaves effectively as phantom DE. The measured cosmological term is $\Lambda = 8\pi G\rho_{\rm vac}$, and hence Λ also runs with H since $\rho_{\rm vac} = \rho_{\rm vac}(H)$. Such a running feature of the VED and Λ occurs in the ΛXCDM too, and in exactly the same form as in Equation (1), but here we have also the dynamics of X, and hence the cosmological solution of the model in terms of the redshift variable is considerably more complicated (J. Grande et al. 2006). Besides, as recently demonstrated in the QFT context, $\rho_{\rm vac}$ has an EOS that departs from -1 (C. Moreno-Pulido & J. Solà Peracaula 2022b), so the "modern version of the ΛXCDM model" actually has two nontrivial EOS parameters, one for the running VED and the other for X, which we call ω_X. These are basic ingredients in our analysis, and for this reason the ΛXCDM fleshes out the theoretical basis inspiring the current work. However, the actual scenario that we will analyze here is model wXCDM (see below). It is simpler than the ΛXCDM but has the same genetic ingredients. We will use it to emulate the basic properties of the latter. The analysis of the cosmic tensions within the full ΛXCDM framework is more demanding and will be presented in a separate work (A. Gómez-Valent & J. Solà Peracaula 2024, in preparation).

ii. wXCDM model. In order to illustrate the possibilities of our composite DE scenario in connection with the cosmological tensions, herein we will use the wXCDM model, a reduced (skeleton) version of the

ΛXCDM. The two models share the X component, but wXCDM mimics the running vacuum feature of ΛXCDM through another dynamical component Y (replacing Λ) and whose EOS, w_Y, can be different from -1. This means that Y does not act as a rigid CC, which is fair enough since, as mentioned before, in the RVM context the VED is dynamical and its EOS (hence that of Λ) actually departs from -1 owing to quantum effects (C. Moreno-Pulido & J. Solà Peracaula 2022b). Thus, in the wXCDM, we have two DE components with potentially different EOS behaviors. Furthermore, as we will see in Section 5, in the best-fit model the X component behaves phantom-like ($\omega_X \lesssim -1$) and the Y component behaves quintessence-like ($\omega_Y \gtrsim -1$). An important point is that X and Y do not act simultaneously: X acts first in the cosmic expansion, and Y acts subsequently. To be precise, X enters only above a transition redshift $z > z_t$ (fitted from the data), while Y enters below that redshift until the current time. No less crucial is the fact that the phantom-like component X actually behaves as PM, therefore with negative energy density ($\Omega_X = \rho_X/\rho_c < 0$) and positive pressure ($p_X > 0$), whereas for the Y component we have $\Omega_Y > 0$, $p_Y < 0$. Notice that the characteristic free parameters of model wXCDM are just (z_t, w_X, w_Y). Indeed, the density parameters for the DE components are not free since, e.g., the value of $\Omega_Y^0 \equiv \Omega_Y(z = 0)$ depends on the fitting values of H_0, ω_b, and $\omega_{\rm dm}$ (see Table 1). In addition, the respective values of Ω_X and of Ω_Y immediately above and below z_t are assumed to be equal in absolute value. This means that $|\Omega_X(z)| = \Omega_Y(z)$ at $z = z_t$. This kind of assumption aims at reducing the number of parameters and is entirely similar to the one made in the Λ_sCDM model; see point (iii) below.

Last but not least, we note that the existence of these two different phases of the DE separated by the redshift z_t is not just an ad hoc assumption since it is found in theoretical contexts such as the stringy RVM approach (N. E. Mavromatos & J. Solà Peracaula 2021a), which points to the existence of transitory domains or bubbles of PM whenever the Universe is approaching a dS epoch (see next sections for more elaboration).

iii. Λ_sCDM model. This is the model recently analyzed with considerable phenomenological success in Ö. Akarsu et al. (2023). Strictly speaking, it is not a composite model since only Λ is involved, although it enters with two signs and in this sense is a composition of two phases of Λ separated also by a transition redshift z_t, which is the characteristic parameter of this model. It is assumed that at that point there is a sudden AdS$-$dS transition from $-\Lambda < 0$ in the upper redshift range to $+\Lambda > 0$ in the lower range, i.e., an abrupt change of sign of Λ at $z = z_t$, but keeping the same absolute value. We refer the reader to the quoted reference for more details.

For convenience, we shall simultaneously provide the fitting results for models (ii) and (iii) under the very same data sources. Together with the standard ΛCDM model, the simultaneous analysis of Λ_sCDM will be useful as a benchmark for rating the performance of the PM approach wXCDM to the cosmological tensions.

3. Phantom Matter and the Energy Conditions of the Cosmic Fluids

Even though PM was first proposed phenomenologically in the old composite cosmological model ΛXCDM (J. Grande et al. 2006, 2007, 2009), more recently it has been put forward on more formal grounds in N. E. Mavromatos & J. Solà Peracaula (2021a), specifically within the context of the stringy RVM approach (see N. E. Mavromatos & J. Solà Peracaula 2021b for a review). Obviously, we need not provide technical details here, and we refer the reader to the aforementioned references. However, we can at least describe the conceptual design of this picture. In a nutshell, it is the following: in a framework of a string-inspired cosmology with primordial gravitational waves (GWs) and gravitational anomalies, which lead to dynamical inflation of RVM type without the need for ad hoc inflaton fields (J. Sola & A. Gòmez-Valent 2015; N. E. Mavromatos & J. Solà Peracaula 2021b), a crucial role is played by the fundamental axion field existing in the gravitational multiplet of string theory, viz., the Kalb–Ramond (KR) axion field $b(x)$, which couples to the gravitational Chern–Simons (gChS) term: $\sim b(x)\, R_{\mu\nu\rho\sigma}\, \widetilde{R}^{\mu\nu\rho\sigma} \equiv b(x) R\, \tilde{R}$, where $\tilde{R}$ denotes the dual of the Riemann tensor. The KR axion and the gChS contribution together obey a peculiar EOS of vacuum type $p = -\rho$ but with negative energy density $\rho < 0$ (hence with positive pressure $p > 0$), which defines the "phantom vacuum" (N. E. Mavromatos & J. Solà Peracaula 2021a). This form of vacuum, however, is merely transitory until the gChS condensates $\langle R\,\tilde{R} \rangle$ become activated through the condensation of primordial GWs, thereby making possible a positive-definite vacuum state energy with effective cosmological "constant" $\Lambda(H) \sim \langle bR\tilde{R} \rangle$. At this juncture, the total pressure and density already involve the combined effect from all the contributions, which makes possible a normal vacuum state with $\rho_{\text{total}} > 0$ and hence with $p_{\text{total}} = -\rho_{\text{total}} < 0$, i.e., a standard dS phase with positive energy density and negative pressure. The latter nevertheless may still be subdued to corrections owing to quantum effects. Interestingly enough, in such a framework the KR axion can be a candidate to dark matter, which provides an additional motivation for this cosmological picture since it could embrace the entire cosmic history.

Thus, a PM-dominated era can be present in the early cosmic evolution near a dS phase, but we should emphasize that it could also reflourish in the late Universe. As shown in S. Basilakos et al. (2019, 2020b, 2020a), due to the generation of chiral matter, which will dominate the Universe at the exit from inflation, at large scales the Universe can recover its Friedmann–Lemaître–Robertson–Walker (FLRW) background profile. This is because the chiral matter fields ensure the cancellation of the gravitational anomalies during the FLRW regime, where they are indeed not observed, as otherwise it would imply a glaring violation of general covariance. However, as soon as we are in the process of exiting the FLRW regime toward a new dS era, we cannot exclude that in successive stages of the cosmic evolution the Universe can be affected by the presence of lurking PM. The reason is that the chiral matter fields will get more and more diluted with the cosmic expansion, and then, due to the incomplete cancellation of the gravitational anomalies, these may eventually resurface near the current quasi-dS era. It is therefore not inconceivable to think of the existence of PM bubbles or domains tunneling now and then into our Universe at relatively close redshift

Table 1
Mean Values and Uncertainties at 68% CL Obtained with the Full Data Set CMB+CCH+SNIa+SH0ES+BAO+$f\sigma_{12}$

Parameter	ΛCDM	wXCDM	Λ_sCDM
ω_b	0.02281 ± 0.00014 (0.02278)	0.02241 ± 0.00013 (0.02260)	$0.02236^{+0.00016}_{-0.00018}$ (0.02232)
ω_{dm}	0.1153 ± 0.0009 (0.1148)	0.1199 ± 0.0010 (0.1196)	$0.1205^{+0.0015}_{-0.0016}$ (0.1216)
$\ln(10^{10}A_s)$	$3.066^{+0.016}_{-0.018}$ (3.080)	3.037 ± 0.014 (3.034)	$3.036^{+0.015}_{-0.016}$ (3.030)
τ	$0.069^{+0.008}_{-0.010}$ (0.076)	0.051 ± 0.008 (0.048)	$0.050^{+0.008}_{-0.009}$ (0.046)
n_s	0.978 ± 0.004 (0.981)	0.967 ± 0.004 (0.969)	$0.966^{+0.004}_{-0.005}$ (0.961)
H_0 (km s^{-1} Mpc^{-1})	$69.82^{+0.41}_{-0.44}$ (70.05)	$72.75^{+0.57}_{-0.71}$ (72.36)	$72.24^{+0.99}_{-0.75}$ (73.82)
z_t	$\cdots$	$1.46^{+0.02}_{-0.01}$ (1.47)	$1.61^{+0.22}_{-0.18}$ (1.47)
w_X	$\cdots$	$-1.16^{+0.13}_{-0.16}$ (−1.16)	$\cdots$
w_Y	$\cdots$	-0.90 ± 0.03 (−0.88)	$\cdots$
Ω_m^0	0.283 ± 0.005 (0.280)	0.269 ± 0.005 (0.272)	0.267 ± 0.005 (0.264)
M	$-19.372^{+0.011}_{-0.012}$ (−19.362)	$-19.273^{+0.015}_{-0.016}$ (−19.282)	$-19.278^{+0.026}_{-0.020}$ (−19.261)
σ_{12}	0.780 ± 0.007 (0.784)	0.776 ± 0.007 (0.772)	$0.782^{+0.007}_{-0.006}$ (0.784)
$\chi^2_{\min}$	4166.76	4107.62	4120.04
ΔDIC	$\cdots$	57.94	40.16
ΔAIC	$\cdots$	53.14	44.72

Note. We show the best-fit values in parentheses. We use the standard notations for the ΛCDM parameters. In the last three lines, we display the values of the minimum χ^2, ΔDIC, and ΔAIC, as defined in Equations (2) and (3), respectively. Positive values of ΔDIC and ΔAIC denote the preference of the new models over the ΛCDM. As can be seen, the preference is extraordinarily high.

ranges before the ultimate dS phase takes over. These bubbles of PM, being endowed with positive pressure $p > 0$, could obviously foster a larger rate of the structure formation, a fact that might explain the overproduction of LSSs at unexpected places and times deep in our past. As we shall next show, this ideology provides an excellent framework for a fit to the overall cosmological data that proves to be (far) better than that of the standard ΛCDM model, provided that we exclusively focus on BAO 2D data in our fit. We refer the reader once more to N. E. Mavromatos & J. Solà Peracaula (2021a) and the review by N. E. Mavromatos & J. Solà Peracaula (2021b) for the details underlying the PM scenario supporting our proposal for solving the tensions. See also N. E. Mavromatos (2022) and the recent developments (N. E. Mavromatos et al. 2024; P. Dorlis et al. 2024). Here we have limited ourselves to a very succinct exposition of the theoretical background, and in the
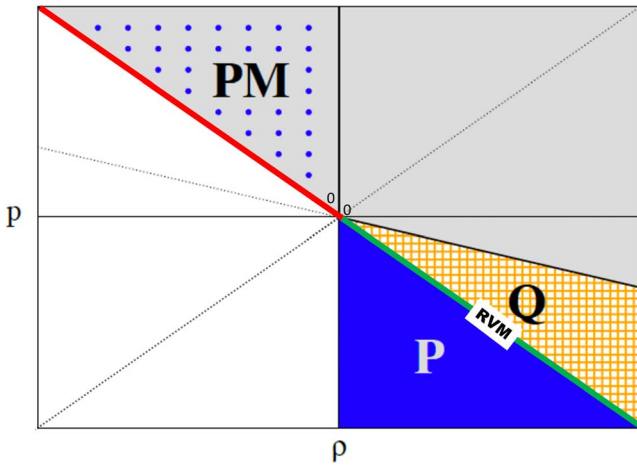
Figure 1. EOS diagram for the energy conditions of the cosmic fluids. The quintessence (Q) region ($-1 < w < -1/3$ with $\rho > 0$, $p < 0$) is marked cross-hatched, and the conventional phantom region ($w \leqslant -1$ with $\rho > 0$, $p < 0$) is the blue sector indicated as P. The gray dotted area corresponds to the peculiar PM region: $w < -1$ with $\rho < 0$ and $p > 0$. Notice that PM satisfies the strong energy condition, $\rho + p \geqslant 0$, $\rho + 3p \geqslant 0$ (all of the gray area), but not the weak energy condition, $\rho \geqslant 0$, $\rho + p \geqslant 0$ (shaded area, except the P and PM sectors). The DE component X in our analysis behaves as PM, whereas the Y component behaves as quintessence. The EOS line $w = -1$ marks off the classical vacuum. The RVM fulfills this EOS only approximately near our time owing to quantum effects (C. Moreno-Pulido & J. Solà Peracaula 2022b). See also J. Grande et al. (2006) and N. E. Mavromatos & J. Solà Peracaula (2021a) for the modern developments on PM.

rest of this work we focus on exploring the phenomenological implications.

Before closing this section, and for the sake of a better contextualization of the PM option within the class of energy conditions, in Figure 1 we show a few of the most common possibilities for the EOS of the cosmic fluids. In it, we particularly highlight the phantom DE (labeled P, in blue) and the PM regions. The latter (marked gray dotted) is far away from the usual phantom DE; it actually lies in its antipodes! These two phantom-like possibilities, both satisfying $w < -1$, are therefore dramatically different and must not be confused. It should also be emphasized that while phantom DE has been amply considered in the literature to describe different features of the DE, including a possible explanation for the H_0 and growth tensions in different frameworks (see the Introduction and references therein), in our approach phantom DE is not used at all. In point of fact, only PM is singled out in an optimal way within our specific proposal for a possible resolution of the cosmological tensions.

4. Data and Numerical Analysis

Let us now come back to the three composite DE models mentioned in Section 2. Leaving model (i) for a separate study (A. Gómez-Valent & J. Solà Peracaula 2024, in preparation), in this work we constrain the DE models (ii) and (iii) making use of the following cosmological data sets:

1. The full Planck 2018 CMB temperature, polarization, and lensing likelihoods (N. Aghanim et al. 2020).
2. The Type Ia supernovae (SNe Ia) contained in the Pantheon+ compilation (D. Brout et al. 2022), calibrated with the cosmic distance ladder measurements of the SH0ES Team (A. G. Riess et al. 2022). We will refer to this data set as SNIa+SH0ES for short.

3. 33 data points on $H(z)$ in the redshift range $z \in [0.07, 1.97]$ from cosmic chronometers (CCH; R. Jiménez et al. 2003; J. Simon et al. 2005; D. Stern et al. 2010; M. Moresco et al. 2012, 2015, 2016; C. Zhang et al. 2014; A. L. Ratsimbazafy et al. 2017; N. Borghi et al. 2022; E. Tomasetti et al. 2023; see also the Appendix of A. Favale et al. 2024a). We employ the corresponding full covariance matrix, as described in M. Moresco et al. (2020).

4. Transverse (aka angular or 2D) BAO data from the literature (G. C. Carvalho et al. 2016, 2020; J. S. Bagla et al. 2017; E. de Carvalho et al. 2018; E. de Carvalho et al. 2021). These types of BAO data are claimed to be less subject to model dependencies, since they are obtained without assuming any fiducial cosmology to convert angles and redshifts into distances to build up the tracer map. The BAO 2D data points are extracted from the two-point angular correlation function or its Fourier transform. In anisotropic (or 3D) BAO analyses, instead, a fiducial cosmology (the standard ΛCDM model) is employed to construct the 3D map in redshift space, potentially introducing some model dependency.[3] It is also worth noticing that despite the fact of being constructed from the same parent catalogs of tracers, angular and anisotropic BAO data exhibit some degree of tension (see, e.g., D. Camarena & V. Marra 2020 and, particularly, the very recent analysis of A. Favale et al. 2024b). In the last study, it is shown that upon excluding the radial component of BAO 3D (which is of course not present in BAO 2D), the "residual" tensions left between the two BAO types can still attain in between 2σ and 4.6σ, depending on the data set used. All in all, not surprisingly, these BAO data tensions may directly impinge in a significant way on the discussion of the cosmological tensions themselves, for the required solution to alleviate them may be conditioned to the specific BAO data type considered in the analysis (A. Gomez-Valent et al. 2024). We should also mention that, in contradistinction to the BAO 3D data, BAO 2D observations still offer room for low-redshift solutions to the Hubble tension while respecting the constancy of the absolute magnitude of SNe Ia (Ö. Akarsu et al. 2023; A. Gomez-Valent et al. 2024). Given, however, the persisting conflict between these two BAO types, our aim here is to remain as model independent as possible in light of the present knowledge, and for this reason we opt for using at this point the kind of BAO data that seem to be less subject to criticism at present (and in this sense that may be more trouble-free), to wit, the BAO 2D type. We leave the detailed comparison with the BAO 3D results for a more comprehensive exposition. A preview

---

[3] This is an important issue to keep in mind, which is in fact at the basis of our approach in the current presentation. It is known that the impact of the fiducial cosmology on the BAO measurements can be small (J. L. Bernal et al. 2020; P. Carter et al. 2020; A. Heinesen et al. 2020; J. Pan et al. 2024), but this is warranted only when such a cosmology is close to the true one. In fact, S. Anselmi et al. (2023) recently argued that these works do not explore a wide enough range of the fiducial parameter values allowed by the measured BAO distances, which are quite far away from the Planck best-fit ΛCDM model. In addition, it is claimed that fitting the two-point correlation function while fixing at the same time the cosmological parameters (and also those entering the correlation function template) at fiducial values might lead to an underestimation of the errors by roughly a factor of two, hence a rather significant potential effect (S. Anselmi et al. 2019).

Table 2
Individual χ_i^2 Contributing to χ_{min}^2, Obtained in the Fitting Analyses for the Various Models with CMB+CCH+SNIa+SH0ES+BAO+$f\sigma_{12}$

χ_i^2	ΛCDM	wXCDM	Λ_sCDM
$\chi_{Planck\_highl\_TTTEEE}^2$	2365.09	2350.78	2350.81
$\chi_{Planck\_lowl\_EE}^2$	404.20	395.91	396.07
$\chi_{Planck\_lowl\_TT}^2$	21.34	25.21	27.80
$\chi_{Planck\_lens}^2$	10.77	9.31	10.74
χ_{CMB}^2	2801.40	2781.21	2785.42
$\chi_{Pantheon+SH0ES}^2$	1312.83	1290.11	1302.21
χ_{BAO}^2	23.87	13.27	13.80
$\chi_{f\sigma_{12}}^2$	15.99	12.68	9.41
χ_{CCH}^2	12.67	10.52	10.20
χ_{min}^2	4166.76	4107.62	4120.04

**Note.** χ_{CMB}^2 contains the total CMB contribution, i.e., it is the sum of all the Planck χ_i^2, which we list in the upper half of the table.

of such a comparative analysis will be nonetheless advanced in the conclusions (see Section 6).[4]

5. The data on LSS at $z \lesssim 1.5$ from the literature (L. Guzzo et al. 2008; Y.-S. Song & W. J. Percival 2009; C. Blake et al. 2011, 2013; T. Okumura et al. 2016; F. Simpson et al. 2016; H. Gil-Marín et al. 2017; F. G. Mohammad et al. 2018; J. Hou et al. 2020; K. Said et al. 2020; F. Avila et al. 2021). These are data points on the observable $f(z)\sigma_8(z)$, with $f(z) = -(1+z)d \ln \delta_m/dz$ the growth rate, $\delta_m = \delta\rho_m/\rho_m$ the matter density contrast, and $\sigma_8(z)$ the rms mass fluctuations at a scale $R_8 = 8\ h^{-1}$ Mpc; see Table 3 of J. Solà Peracaula et al. (2023). These data points, though, are taken by the observational groups using a fiducial cosmology with $h \sim 0.67$, which translates into measurements at a characteristic scale of $R \sim 12$ Mpc. Here, in contrast, we adhere to the reasoning and practice of A. G. Sanchez (2020) and A. Semenaite et al. (2022, 2023), and we treat these observations as data points on $f(z)\sigma_{12}(z)$, using a Fourier-transformed top-hat window function $W(kR_{12})$ in the computation of $\sigma_{12}(z)$. The advantage, as emphasized by these authors, is that the scale $R_{12} = 12$ Mpc is independent of the parameter h.

We compute all the cosmological observables using a modified version of the Einstein–Boltzmann code CLASS (D. Blas et al. 2011; J. Lesgourgues 2011), and explore and constrain the parameter space of the various models using the Metropolis–Hastings algorithm (N. Metropolis et al. 1953; W. K. Hastings 1970) implemented in MontePython (B. Audren et al. 2013; T. Brinckmann & J. Lesgourgues 2019). The resulting Monte Carlo Markov chains are analyzed with the Python code GetDist (A. Lewis 2019). Our main

---

[4] The extended discussion, including an explicit comparison between the results obtained from BAO 2D and BAO 3D data, as well as the computational details of the present work, will be disclosed in a forthcoming comprehensive study (A. Gómez-Valent & J. Solà Peracaula 2024, in preparation).
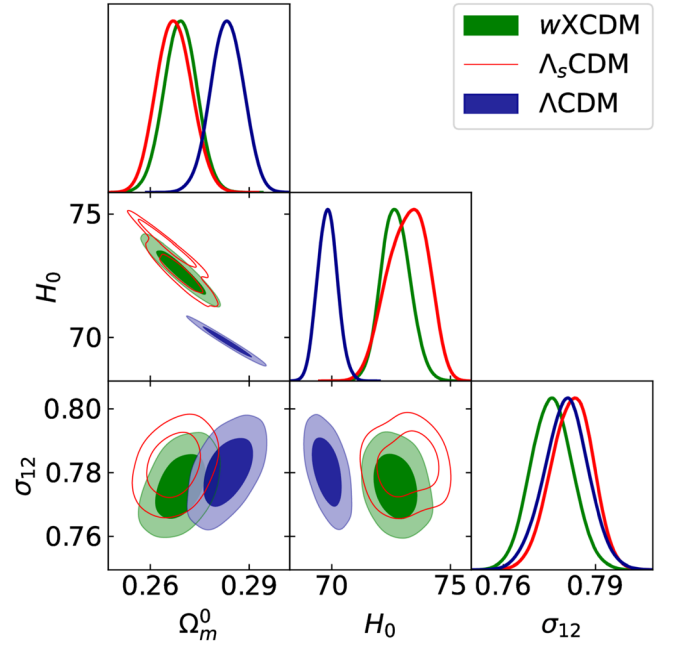
Figure 2. Contour plots at 68% and 95% CL and the corresponding 1D posterior distributions for some of the parameters that are relevant in the discussion of the cosmological tensions, for all the models under study. H_0 is given in km s^{-1} Mpc^{-1}. The complete triangle plot is presented in Figure 4.
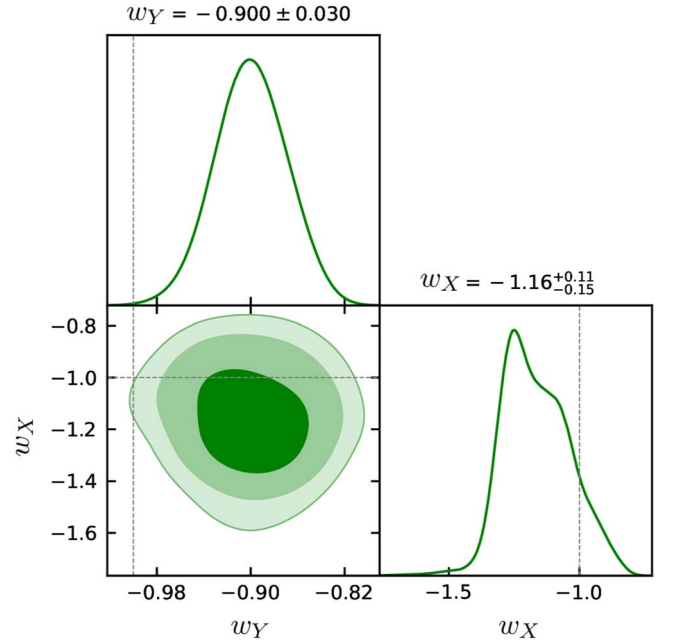

Figure 3. Confidence regions in the w_Y-w_X plane of the wXCDM model, and the corresponding 1D posterior distributions. The dotted lines are set at $w_Y = -1$ and $w_X = -1$. The intersection of the horizontal and vertical lines in the contour plot corresponds to the Λ_sCDM model, which falls $\gtrsim 3\sigma$ away from the preferred region of the wXCDM. See the main text for further comments.

numerical results are presented in Tables 1 and 2 and in the triangle plots of Figures 2, 3 and 4

In Table 1 we not only list the mean of the various parameters, with their uncertainties and best-fit values, but also report the minimum values of χ^2 obtained for each model and the difference between the deviance information criterion (DIC; D. J. Spiegelhalter et al. 2002) and the Akaike information criterion (AIC; H. Akaike 1974) found between the
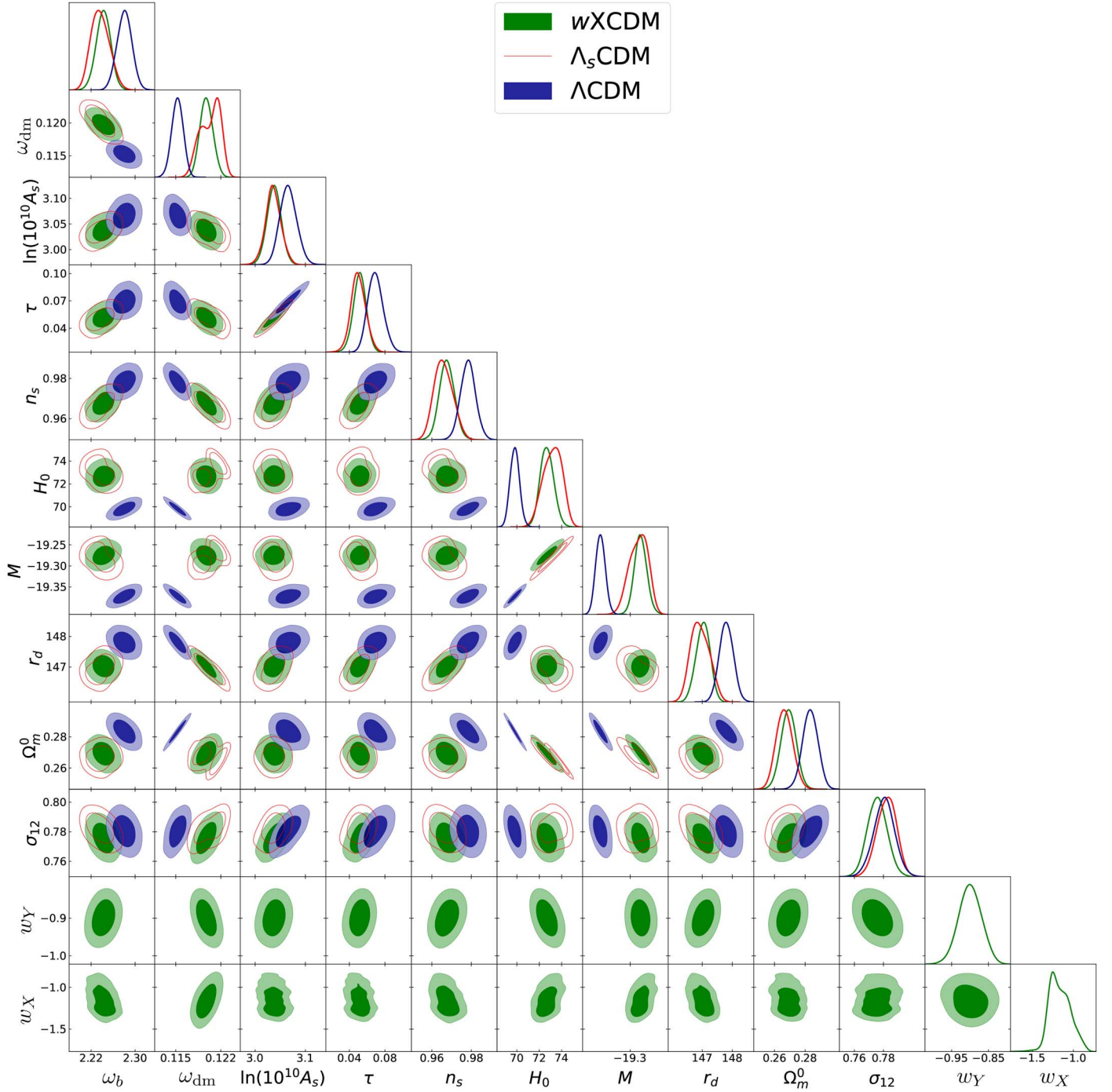
Figure 4. Full triangle plot for the various models studied in this paper. We show the constraints at 68% and 95% CL in all the relevant planes of the parameter spaces, together with the individual 1D posterior distributions. H_0 is given in km s^{-1} Mpc^{-1}.

composite DE models and ΛCDM, which we treat as our fundamental benchmark model. These differences read $\Delta\mathrm{DIC} \equiv \mathrm{DIC}_{\Lambda\mathrm{CDM}} - \mathrm{DIC}_i$ and $\Delta\mathrm{AIC} \equiv \mathrm{AIC}_{\Lambda\mathrm{CDM}} - \mathrm{AIC}_i$, respectively, with i referring to wXCDM or Λ_sCDM. Both criteria penalize the use of additional parameters and can be regarded as a rigorous mathematical implementation of Occam's razor. The DIC is defined as

$$\mathrm{DIC} = \chi^2(\bar{\theta}) + 2p_D, \qquad (2)$$

with $p_D = \overline{\chi^2} - \chi^2(\bar{\theta})$ the effective number of parameters in the model, $\overline{\chi^2}$ the mean value of χ^2, and $\bar{\theta}$ the mean of the

parameters that are left free in the Monte Carlo analysis. Similarly, AIC is defined as

$$\mathrm{AIC} = \chi^2_{\min} + 2n_p, \qquad (3)$$

with n_p the number of free parameters entering the fit. We note that the above formula is a good approximation when the number of data points entering the fit is much larger than n_p, which is certainly the case here. With our definition, a positive difference of these information criteria implies that the composite DE models perform better than the ΛCDM, whereas negative differences imply just the opposite.

According to the usual jargon of the information criteria, if $0 \leqslant \Delta\mathrm{DIC} < 2$, it is said that one finds weak evidence in favor of the new model under test (in this case, the composite DE models under scrutiny), as compared to the standard model. If $2 \leqslant \Delta\mathrm{DIC} < 6$, we speak, instead, of positive evidence. If $6 \leqslant \Delta\mathrm{DIC} < 10$, there is strong evidence in favor of the composite DE models, while for $\Delta\mathrm{DIC} > 10$ we may legitimately conclude that there is very strong statistical evidence supporting the new model or models against the standard ΛCDM. Analogous considerations can be made using AIC, of course. DIC is considered to be a more accurate information criterion, since it incorporates the information encapsulated in the full Markov chains. However, for the sake of generality and to explicitly show the consistency between these two criteria, we display the results obtained from both criteria at the same time in our Table 1.

5. Discussion

As we have mentioned, bubbles of PM are connected with the process of attaining the dS era both in the early Universe and in the late Universe. During the transit from the provisional phantom vacuum into the true and stable (dS) vacuum, the PM bubbles being tunneled in the late Universe are characterized by positive pressure and hence offer a fertile field for the growing of unsuspected structures. This mechanism, therefore, provides a tantalizing theoretical framework capable of explaining physically the appearance of a late-time AdS epoch (or epochs) before the usual dS epoch is eventually attained.[5] In point of fact, we do not expect that these PM bubbles are perfect AdS phases (nor that the subsequent stage is necessarily characterized by a rigid $\Lambda > 0$), and for this reason we have left the EOS parameter w_X as a free parameter, whose fitted value turns out to be $w_X \simeq -1.16$ (see Table 1), although with $\rho_X < 0$ (in contrast to conventional phantom DE). Since the bubble is transitory, the ensuing DE phase below z_t follows a different equation of state (EOS), which we fit to be quintessence-like: $w_Y \simeq -0.90$ (see Table 1). We have performed a comparative fitting analysis of the wXCDM and Λ_sCDM scenarios using the same data sets and have found a significantly better fit quality for the PM scenario, as shown in Table 1. We shall come back to these results in a moment.

The PM phase or phases with negative energy density and positive pressure are left behind during the cosmic evolution at relatively large redshifts of order 1–10, and in these places they can leave a sort of oasis rich of LSSs, whereas the consecutive evolution (closer to our time) flips into the quintessence regime. Although we have used an abrupt θ-function behavior to connect the two EOS regimes, in actual fact the process is continuous since the Chern–Simons condensates eventually dominate and restore the normal vacuum phase with positive energy. To better understand, in a quantitative way, how the PM bubbles with positive pressure may enhance the formation of (unsuspected) LSSs in the relatively distant past, it is useful to analyze the differential equation for the matter density contrast in the presence of PM. This is a key aspect of the role

played by PM for potentially helping to solve the cosmological tensions. Before the transition at z_t (i.e., for $z > z_t$), the equation for δ_m reads[6]

$$\delta_m'' + \frac{3}{2a}(1 - \Omega_X(a)w_X)\delta_m' - \frac{3}{2a^2}(1 - \Omega_X(a))\delta_m = 0, \quad (4)$$

with the primes denoting derivatives with respect to the scale factor. PM has negative energy density ($\Omega_X < 0$) and positive pressure (due to $w_X < -1$), and therefore it induces a decrease of the friction term and an increase of the Poisson term (the last one) in Equation (4). Both effects are in harmony and therefore bring about, given some fixed initial conditions, a net enhancement of the structure formation processes in the PM bubbles. Notice that this would not occur for ordinary phantom DE or for quintessence (see Figure 1), for which the friction term gets enhanced and the Poisson term gets suppressed, i.e., just the opposite situation to PM. This conspicuous impact on LSS is therefore unique to PM since there is no other cosmic fluid capable of matching such an achievement in the EOS diagram of Figure 1.

Moreover (and this is crucial to understanding how the H_0 tension can be potentially cured in the PM framework), because the energy of the X entity is negative, $\Omega_X < 0$ (and nonnegligible at high redshift), it enforces a higher value of the expansion rate H in the quintessence stage in order to preserve the angular diameter distance to the last scattering surface, which is essentially fixed from the very precise measurement of θ_* (the angular size of the sound horizon) by Planck (N. Aghanim et al. 2020) and the standard physics before recombination (A. Gomez-Valent et al. 2024). This explains on plausible physical grounds why H_0 is found larger than in the ΛCDM in our PM scenario. Quantitatively, our value of H_0 (see Table 1) is in full agreement with that of SH0ES ($H_0 = 73.04 \pm 1.04 \, \mathrm{km\,s^{-1}\,Mpc}$; A. G. Riess et al. 2022) to within $\lesssim 0.25\sigma$. The Hubble tension is therefore virtually washed out, even when expressed in terms of the absolute magnitude of SNe Ia: our fitted value of M and that of SH0ES ($M = 19.253 \pm 0.027$ mag) differ by only $\sim 0.6\sigma$. At the same time, the rate of LSS formation becomes suppressed below $z_t \sim 1.5$ during the quintessence-like regime, as explained above, which is also in accordance with the observations. In Table 1 and, more graphically, in Figure 2, we can see that the amplitude of the power spectrum at linear scales that is preferred by the data is pretty similar in all the models under study. Indeed, in all cases we find values of $\sigma_{12} \sim 0.78$. However, at a finer level of scrutiny, Table 2 tells us that the wXCDM is better able to better the LSS data than the ΛCDM, which means that the composite DE model is able to produce lower values of $f(z)\sigma_{12}(z)$ and, hence, of $f(z)$ since σ_{12} remains stable in the various models. This can again be understood by looking at the equation for the density contrast, whose form at $z < z_t$ is identical to Equation (4), but with the replacements $\Omega_X \to \Omega_Y$ and $w_X \to w_Y$,

$$\delta_m'' + \frac{3}{2a}(1 - \Omega_Y(a)w_Y)\delta_m' - \frac{3}{2a^2}(1 - \Omega_Y(a))\delta_m = 0. \quad (5)$$

---

[5] This is in contradistinction to the alternative Λ_sCDM scenario analyzed in Ö. Akarsu et al. (2023), although theoretical attempts at justifying it have appeared recently (O. Akarsu et al. 2024a, 2024b; L. A. Anchordoqui et al. 2024a, 2024b).

[6] As indicated, we shall not provide computational details here. For a full-fledged exposition, including the complete set of coupled perturbation equations of the wXCDM model, see A. Gómez-Valent & J. Solà Peracaula (2024, in preparation).

It is clear from Figure 2 that the values of the matter density parameter $\Omega_m^0 = \Omega_m(a = 1)$ in the wXCDM are way smaller than those in the ΛCDM. This obviously translates into larger values of $\Omega_Y(a) > 0$ (higher than Ω_Λ^0 in the ΛCDM), which makes matter fluctuations grow less efficiently in our model after the transition (at $z < z_t$), a welcome feature that is rightly aligned for potentially also solving the growth tension within the PM picture. As previously mentioned, despite the presence of PM in the past, the value of σ_{12} in wXCDM is not significantly different ($\sim 0.4\sigma$) from that of ΛCDM. This is due to the slower increase of matter fluctuations in the late-time Universe and the smaller value of the amplitude of primordial fluctuations (A_s) found in wXCDM, which somehow compensate for the presence of PM at $z > z_t$ and keep the value of σ_{12} stable (see again Table 1, as well as Figure 4).

From our numerical analysis we can see that both models wXCDM and Λ_sCDM offer a dramatic reduction of the cosmological tensions. This is apparent from Table 1. One could say that the Hubble and growth tensions disappear in these models. However, there are also important quantitative (and conceptual) differences between them. In terms of the information criteria, we find that the two models wXCDM and Λ_sCDM are very strongly preferred over ΛCDM. Numerically, however, the wXCDM solution provides a significantly better global fit. For this model we find ΔDIC, ΔAIC $\gtrsim 55$, whereas for Λ_sCDM we obtain ΔDIC, ΔAIC $\gtrsim 40$. The difference of 15 units is quite substantive and indicates (in the common parlance of the information criteria) that there is very strong evidence that model wXCDM is preferred over model Λ_sCDM (for the same data). Worth noticing is also the fact that our own results for Λ_sCDM agree with those originally reported in Ö. Akarsu et al. (2023), despite the existing differences in the data sets employed in the two analyses. Apart from our using data on CCH, which were not considered in Ö. Akarsu et al. (2023), we employ data on $f(z)\sigma_{12}(z)$ instead of the weak-lensing (WL) data from KiDS. We do not use WL data in our analysis in order not to compromise the computation of the nonlinear matter power spectrum, which might not be sufficiently well under control in the models under study. Our fitting results, though, are completely consistent with theirs, leading also to similar values of $S_8 \sim 0.78$ (as we have checked), the latter being a more natural LSS parameter in the context of WL analyses, but not in our approach.

Perhaps the most remarkable outcome of our analysis is that, in light of the overall fit quality of our results, which lead to such an outstanding support to the composite DE models from the information criteria, it should be fair to conclude that the standard ΛCDM model appears to be comparatively ruled out at a very high CL. However, once more, we have to warn the reader that, in principle, such a conclusion ensues under the assumption that only BAO 2D has been employed in our analysis (see, however, the additional comments in Section 6). In an attempt to further understand the great success of the numerical fits from the composite DE models in Table 1, let us analyze the degree of impact from each data source. The quantitative influence of each data source can be inferred directly from Table 2, where a detailed breakdown of the different contributions to χ^2 is reckoned. The angular/transversal BAO data certainly contribute in a significant way, as could be expected from the analysis of A. Gomez-Valent et al. (2024). However, it is by no means the leading contribution, as it is responsible for $\sim 18\%$ of the success.

A close inspection of the mentioned table shows that the composite DE models actually beat the ΛCDM in every single observable, and not only in those driving the tensions. Particularly noticeable is the sizable impact from such a solid asset of basic data as the CMB and SNIa+SH0ES observations, which are responsible for about 70% of our successful fitting result, whereas the influence from LSS data is less than 10%, and, finally, that of CCH is marginal (a few percent). The bulk of the successful fit, therefore, relies on the most fundamental cosmological data, which is remarkable. Not only is the ΛCDM unable to explain the large value of H_0 measured by SH0ES or to further slow down the growth rate at low redshift, but it also introduces other tensions, e.g., with the value of the (reduced) cosmological matter parameter $\omega_m = \omega_b + \omega_{dm}$ that is preferred by the Planck data in models that assume standard model physics before the decoupling of the CMB photons, $\omega_m = 0.142 \pm 0.001$ (N. Aghanim et al. 2020). The latter is fully consistent with the wXCDM value ($\omega_m = 0.142 \pm 0.001$) but differs by 2.8σ with the one inferred in the standard ΛCDM ($\omega_m = 0.138 \pm 0.001$). All that said, we remark that the BAO data indeed play a momentous role in the H_0 tension, for despite the fact that the overall fit with composite DE does substantially improve using any of the two variants of BAO, the specific relief of the H_0 tension hinges dramatically on the particular sort (2D or 3D) of BAO that is employed (see Section 6).

We should emphasize that the global outperformance of the composite DE models under study as compared to the ΛCDM is obtained after duly penalizing the use of extra parameters in them. This is of course implemented automatically by the information criteria, as explained above. Thus, for the Λ_sCDM there is the transition redshift z_t as a new parameter with respect to the ΛCDM, whereas for the wXCDM we have, in addition, the two EOS parameters w_X and w_Y for the two phases of the DE. Despite the presence of these extra parameters, Occam's razor (formalized through the verdict of the information criteria) still bestows exceptional preference for the composite models over the concordance model. This is the first important conclusion of our analysis, which suggests that the composite nature of the DE could be a fact. The second is that the relative differences between the two composite models under scrutiny, namely $\mathrm{DIC}_{\Lambda_s\mathrm{CDM}} - \mathrm{DIC}_{w\mathrm{XCDM}} = 17.78$ and $\mathrm{AIC}_{\Lambda_s\mathrm{CDM}} - \mathrm{AIC}_{w\mathrm{XCDM}} = 8.42$, clearly point to a rather keen preference for wXCDM over Λ_sCDM under the same data.

Focusing now on the wXCDM parameters, in Figure 3 we show the constraints obtained in the EOS plane w_Y-w_X, which involves two of the characteristic new parameters of the wXCDM model (the third one being z_t, shared with Λ_sCDM). The central value of $w_X = -1.16$ falls in the phantom region (in fact, PM region since $\Omega_X < 0$) but is compatible with -1 at $\sim 1\sigma$ CL There is, in contrast, a nonnegligible ($\sim 3.3\sigma$) preference for a quintessence-like evolution of the DE for the low redshift range nearer to our time ($z < z_t$): $w_Y = -0.90 \pm 0.03$ (see also Figure 3). The preference that we find for quintessence-like behavior in this region can be contrasted with the situation in the Λ_sCDM, where a rigid Λ-term is assumed below the transition redshift (also above that redshift, with $\Lambda \rightarrow -\Lambda$). Now the fact that our fit with model wXCDM proves significantly better than with model Λ_sCDM (as commented above) suggests that indeed the quintessence option in the low redshift range is strongly preferred. Our result aligns perfectly well with the one obtained from the analysis of the Pantheon+ data in the context of the flat wCDM parameterization

(D. Brout et al. 2022), which showed that SN Ia data alone lead to an EOS parameter $w = -0.89 \pm 0.13$ after marginalizing over Ω_m^0. This marginalized result, though, is still compatible with a CC ($w = -1$). To explain why our case is more focused on the quintessence domain, let us note that for wXCDM we find a tight constraint on the matter density parameter, strongly favoring the region of small values, $\Omega_m^0 = 0.269 \pm 0.005$. This is induced by two facts: (i) CMB prefers values of $\omega_m \sim 0.142$ in models with standard pre-recombination physics, and (ii) the large values of $H_0 \sim 73 \, \mathrm{km \, s^{-1} \, Mpc}$ measured by SH0ES. Combining the aforementioned tight constraint on Ω_m^0 with the constraints in the $w - \Omega_m^0$ plane obtained for the wCDM from the analysis of the Pantheon+ data alone (see the cyan contours in Figure 9 of D. Brout et al. 2022), we can break the existing degeneracy in that plane and explain the $\gtrsim 3\sigma$ evidence for quintessence DE that we find within the wXCDM for the low redshift range. We point out that, for the conventional wCDM parameterization (i.e., without the X component), such low values of Ω_m^0 are not favored by Planck, since they are in tension with the angular diameter distance to the last scattering surface (see again Figure 9 of D. Brout et al. 2022). Remarkably, this problem can be fully averted in the wXCDM model owing precisely to the concurrence of the X component, which can act as PM in the high-redshift stretch $z > z_t$ and compensate for the decrease of the contribution to the angular diameter distance in the low-redshift domain. On the other hand, in the Λ_sCDM case we also find similar low values of Ω_m^0. However, to retrieve this model from the wXCDM, we have to set w_Y to -1 (rigid CC),[7] so the Λ_sCDM falls outside the 3σ region obtained with wCDM using only SN Ia data (D. Brout et al. 2022). This issue is also solved in the wXCDM and explains the improvement found with respect to the Λ_sCDM model. The full 5 yr data set of high-redshift SNe Ia from the Dark Energy Survey (T. M. C. Abbott et al. 2024) and the Union3 SN Ia compilation (D. Rubin et al. 2023) will most likely increase the aforesaid signal, since they also find constraints in the region of interest, which read $(\Omega_m^0, w) = (0.264^{+0.074}_{-0.096}, -0.80^{+0.14}_{-0.16})$ and $(\Omega_m^0, w) = (0.244^{+0.092}_{-0.128}, -0.735^{+0.169}_{-0.191})$, respectively. Hence, it will be of utmost importance to study the impact of these data sets in future analyses. In addition, our fitting results for wXCDM are compatible at roughly $\sim 1\sigma$ with those recently reported by DESI using the wCDM parameterization (A. G. Adame et al. 2024). Although 2 of the 12 DESI BAO data points (specifically those obtained with Lyα quasars (QSOs) at $z_{\rm eff} = 2.33$) lie outside the quintessence region identified in our wXCDM model, the bulk of the DESI points lie below $z = 1.5$. The exclusion of the Lyα QSO data points in their fitting analysis might even improve further the compatibility with our findings. Additionally, some recent analyses using DESI data to reconstruct the DE density have found hints of negative values at $z > 1.5$ (R. Calderón et al. 2024; L. Orchard & V. H. Cárdenas 2024). Since the DESI data are derived from anisotropic (3D) BAO, exploring future angular BAO data from DESI (if available) and comparing them with the BAO 3D data would be an interesting avenue for further research.

6. Conclusions

In this paper we have addressed a possible solution to the cosmological tensions within a simplified version of the old

existing ΛXCDM framework (J. Grande et al. 2006, 2007, 2009), which was born in the theoretical arena of the RVM (see J. Solà 2013; J. Solà Peracaula 2022, and references therein). Our modern approach benefits from the new theoretical developments in the context of the stringy version of the RVM (StRVM; N. E. Mavromatos & J. Solà Peracaula 2021b, 2021a). The entity X that is involved in the ΛXCDM need not be a fundamental field but can display a PM behavior, which in the StRVM is predicted to appear in the cosmic transit to the dS phase. The PM regime is, therefore, only transitory and acts as a temporary stage with negative energy and positive pressure. It can be a pure AdS phase, but in general its EOS w_X is not necessarily -1, although it must satisfy $w_X \lesssim -1$. In this work we have contented ourselves with a simplified version of the full ΛXCDM, which we have called the wXCDM. We have utilized a robust data set, which includes the Pantheon+ compilation of SNe Ia, cosmic chronometers, transverse BAO, LSS data, and the full CMB likelihood from Planck 2018. As warned previously, our exclusive use of transverse (2D) BAO aims at maximally mitigating the model-dependent effects that may be introduced on using anisotropic (3D) BAO, according to some published studies. No similar issues have been identified in BAO 2D, and hence we have focused here on using only uncontested BAO data, with the hope that the situation with BAO 3D will be completely clarified in the near future (see, however, the additional comments below).

Using the wXCDM and the aforementioned data configuration, we find that the PM phase shows up above a transition redshift $z_t \simeq 1.5$ (see Table 1). For $z > z_t$ the PM behavior is rapidly washed out since its energy density fraction becomes smaller and smaller in the past. On the other hand, its effect toward our time ($z < z_t$) becomes erased by the progressive appearance of the Chern–Simons condensates, which are responsible for eventually establishing a steady $\Lambda = \mathrm{const.} > 0$ regime (N. E. Mavromatos & J. Solà Peracaula 2021a). For this reason, in practice, the appearance of a PM phase is confined to a bubble of spacetime, which is left behind. However, in that space and time new structures can emerge, being completely unsuspected in the context of the standard model. The PM bubbles that are met within the stringy RVM formulation originate as a result of a "phantom vacuum" phase, which emerges in the Universe when the expansion heads toward the next dS epoch. While the implications of this fact for the early Universe were considered previously (N. E. Mavromatos & J. Solà Peracaula 2021a), here we have extended this phenomenon to the late Universe. In both cases the PM bubbles are localized spacetime events. They can only occur as tunneling attempts to establish the phantom vacuum (N. E. Mavromatos & J. Solà Peracaula 2021a) with positive pressure and negative energy: $p = -\rho > 0$. Below the transition redshift, the PM phase ceases to occur and the field Y (viz., the would-be running VED in the full ΛXCDM; J. Grande et al. 2006) takes its turn with a new effective EOS, which is fitted to be of quintessence type ($w_Y \gtrsim -1$) at $\sim 3.3\sigma$ CL. As a matter of fact, this is the effective form of DE that is expected in our most recent past ($z < 1.5$) within the wXCDM, although from a more fundamental level it could just be running vacuum energy with $\nu_{\rm eff} > 0$ in the full ΛXCDM model; see Equation (1). The observed DE should thereupon be dynamical, and this important conclusion is in stark contrast with the alternative Λ_sCDM scheme analyzed in Ö. Akarsu et al. (2023), in which below the transition redshift

---

[7] Note that the Λ_sCDM model can be viewed as just the single point $(w_Y, w_X) = (-1, -1)$ in the wXCDM parameter space of Figure 3.

there is a rigid and positive cosmological term $\Lambda = $ const. Actually, no possible time dynamics for the DE is available for the Λ_sCDM, neither above nor below z_t. On this account, the picture emerging from the wXCDM looks more consistent with the first data release by DESI (A. G. Adame et al. 2024), which points to dynamical DE. As noted in the Introduction, the fashionable conclusion about potential evidence of time-evolving DE is actually well in consonance with previous phenomenological studies of the RVM from several years ago, which were based on a pretty large set of cosmological data of various sorts. These early detailed studies already anticipated significant signs of dynamical DE at 3σ–4σ CL (J. Solà et al. 2015, 2017; J. Solà Peracaula et al. 2017, 2018a, 2018b; A. Gómez-Valent & J. Solà Peracaula 2018). The current work aligns well with these studies, which were like a harbinger of the dynamical character of the DE emerging from the analysis of a large body of observational data. But at the same time, it leads to further insight into possibly new qualitative properties of the DE, in particular its preference for undergoing a sign flip at a nearby transition redshift, thus adopting a sort of chameleonic nature around that transition point, for the DE appears phantom-like first (viz., PM) and subsequently shows up as effective quintessence near our time (as recently observed by DESI). This combined feature of the DE optimizes to a large extent the quality fit to the overall cosmological data as compared to the ΛCDM. While this positive feature holds true for both types of BAO, it does not help resolve the H_0 tension.

All in all, model wXCDM potentially offers a rich conceptual framework for our understanding of the physical phenomena that may be involved. In the wXCDM, the formation of PM bubbles is induced by quantum fluctuations associated with the nearing of the Universe toward a dS phase. The phenomenon need not be unique: the bubbles of PM could well be operating more than once at earlier times on the same physical grounds, which would trigger an anomalous out-growth of structures at even higher redshifts, say, in the range $z \sim 5$–10. This might explain the appearance of the LSSs recently spotted at unusually high redshifts by the JWST mission (S. A. Adil et al. 2023; I. Labbé et al. 2023; N. Menci et al. 2024). Such LSS "anomalies," which find no explanation in the ΛCDM, might also be described within the current proposal since they can be conceived as being the earliest bubbles of PM popping up in the late Universe, corresponding probably to the first tunneling attempts anticipating the eventual dS phase near our time. This is reasonable, given the fact that the tunneling process toward the final dS era should be gradual, exactly as in the early Universe (N. E. Mavromatos & J. Solà Peracaula 2021a).

Last but not least, as promised, we would like to advance here, if only very briefly, the outcome of the preliminary analysis performed with BAO 3D data. Our extended study has revealed that the wXCDM model with BAO 3D (replacing BAO 2D) data improves once more (and quite significantly) the overall fit to the cosmological data as compared to the ΛCDM (see A. Gómez-Valent & J. Solà Peracaula 2024, in preparation). This should not come as a big surprise, if we take into account our discussion in the previous section, where we have shown by appealing to Table 2 that the composite DE models beat the ΛCDM in every single observable, not only in those driving the tensions. This means that the composite feature of the DE proves really fruitful to better accommodate the various sources of cosmological data. This is remarkable in

the first place, for it means that the superiority of the composite DE models over the ΛCDM is not compromised at present by the particular type (2D or 3D) of BAO data used, despite them being currently under some tension (D. Camarena & V. Marra 2020; A. Favale et al. 2024b; A. Gomez-Valent et al. 2024). Notwithstanding this relevant fact, which holds good for the global fit involving all sorts of cosmological data, we should not underemphasize that, insofar as concerns the H_0 tension itself, the fit with BAO 3D data proves unable to match the efficiency of the BAO 2D fit. Specifically, with BAO 3D the H_0 tension persists at a level of $\sim 2.9\sigma$ (no longer at the insignificant level of 0.25σ like in the BAO 2D case). Thus, while it is true that with BAO 3D the H_0 tension gets somewhat reduced from the large initial value ($\sim 5\sigma$ CL), it still remains sizable. In contrast, we find that the growth tension is less affected. All in all, a final solution to the cosmological tensions —above all to the H_0 tension—is still being compromised by a lack of consistency between the two sources of BAO, angular and anisotropic. The systematic exposition of the results with BAO 3D, along with the quantitative differences with respect to the analysis using BAO 2D, is beyond the scope of this work, and its presentation is left for a separate publication (A. Gómez-Valent & J. Solà Peracaula 2024, in preparation).

At the end of the day, it is encouraging to realize that the physics involved in the PM scenario presented here for a potential solution to the cosmological tensions might ultimately stem from (dynamical) quantum vacuum phenomena, which gives hope for eventually achieving a deeper understanding of the cosmological evolution of the Universe from fundamental physics. Whether this is actually the case or not will depend, of course, on the eventual resolution of the BAO tension itself, which appears to be the main stumbling block for the ultimate understanding of the problem.

ORCID iDs

Adrià Gómez-Valent ● https://orcid.org/0000-0002-2922-2622
Joan Solà Peracaula ● https://orcid.org/0000-0002-5295-8275

References

Abbott, T. M. C., Acevedo, M., Aguena, M., et al. 2024, ApJL, 973, L14
Abdalla, E., Abellán, G. F., Aboubrahim, A., et al. 2022, JHEAp, 34, 49
Adame, A. G., Aguilar, J., Ahlen, S., et al. 2024, arXiv:2404.03002
Ade, P. A. R., Aghanim, N., Arnaud, M., et al. 2016, A&A, 594, A13
Adil, S. A., Mukhopadhyay, U., Sen, A. A., & Vagnozzi, S. 2023, JCAP, 10, 072
Aghanim, N., Akrami, Y., Ashdown, M., et al. 2020, A&A, 641, A6

Akaike, H. 1974, ITAC, 19, 716
Akarsu, Ö., Barrow, J. D., Escamilla, L. A., & Vazquez, J. A. 2020, PhRvD, 101, 063528
Akarsu, O., De Felice, A., Di Valentino, E., et al. 2024a, arXiv:2406.07526
Akarsu, O., De Felice, A., Di Valentino, E., et al. 2024b, arXiv:2402.07716
Akarsu, Ö., Di Valentino, E., Kumar, S., et al. 2023, arXiv:2307.10899
Akarsu, Ö., Kumar, S., Özülker, E., & Vazquez, J. A. 2021, PhRvD, 104, 123512
Alestas, G., Camarena, D., Di Valentino, E., et al. 2022, PhRvD, 105, 063538
Alestas, G., Kazantzidis, L., & Perivolaropoulos, L. 2021, PhRvD, 103, 083517
Anchordoqui, L. A., Antoniadis, I., & Lust, D. 2024a, PhRvB, 855, 138775
Anchordoqui, L. A., Antoniadis, I., Lust, D., et al. 2024b, arXiv:2404.17334
Anselmi, S., Corasaniti, P.-S., Sanchez, A. G., et al. 2019, PhRvD, 99, 123515
Anselmi, S., Starkman, G. D., & Renzi, A. 2023, PhRvD, 107, 123506
Audren, B., Lesgourgues, J., Benabed, K., & Prunet, S. 2013, JCAP, 1302, 001
Avila, F., Bernui, A., de Carvalho, E., & Novaes, C. P. 2021, MNRAS, 505, 3404
Avsajanishvili, O., Chitov, G. Y., Kahniashvili, T., Mandal, S., & Samushia, L. 2024, Univ, 10, 122
Bagla, J. S., Engineer, S., Alcaniz, J. S., et al. 2017, FTP, 187, 11
Basilakos, S., Mavromatos, N. E., & Solà Peracaula, J. 2019, IJMPD, 28, 1944002
Basilakos, S., Mavromatos, N. E., & Solà Peracaula, J. 2020a, PhLB, 803, 135342
Basilakos, S., Mavromatos, N. E., & Solà Peracaula, J. 2020b, PhRvD, 101, 045001
Bernal, J. L., Smith, T. L., Boddy, K. K., & Kamionkowski, M. 2020, PhRvD, 102, 123515
Blake, C., Baldry, I. K., Bland-Hawthorn, J., et al. 2013, MNRAS, 436, 3089
Blake, C., Brough, S., Colless, M., et al. 2011, MNRAS, 415, 2876
Blas, D., Lesgourgues, J., & Tram, T. 2011, JCAP, 1107, 034
Borghi, N., Moresco, M., & Cimatti, A. 2022, ApJL, 928, L4
Brinckmann, T., & Lesgourgues, J. 2019, PDU, 24, 100260
Brout, D., Scolnic, D., Popovic, B., et al. 2022, ApJ, 938, 110
Calderón, R., Gannouji, R., L'Huillier, B., & Polarski, D. 2021, PhRvD, 103, 023526
Calderón, R., Lodha, K., Shafieloo, A., et al. 2024, arXiv:2405.04216
Camarena, D., & Marra, V. 2020, MNRAS, 495, 2630
Carter, P., Beutler, F., Percival, W. J., et al. 2020, MNRAS, 494, 2076
Carvalho, G. C., Bernui, A., Benetti, M., Carvalho, J. C., & Alcaniz, J. S. 2016, PhRvD, 93, 023530
Carvalho, G. C., Bernui, A., Benetti, M., et al. 2020, APh, 119, 102432
Dai, M., Freeman, W., Laiho, J., Schiffer, M., & Unmuth-Yockey, J. 2024, arXiv:2408.08963
de Carvalho, E., Bernui, A., Avila, F., Novaes, C. P., & Nogueira-Cavalcante, J. P. 2021, A&A, 649, A20
de Carvalho, E., Bernui, A., Carvalho, G. C., et al. 2018, JCAP, 04, 064
Di Valentino, E., Anchordoqui, L. A., Akarsu, Ö., et al. 2021a, APh, 131, 102605
Di Valentino, E., Anchordoqui, L. A., Akarsu, Ö., et al. 2021b, APh, 131, 102604
Dorlis, P., Mavromatos, N. E., & Vlachos, S.-N. 2024, PhRvD, 110, 063512
Favale, A., Dainotti, M. G., Gómez-Valent, A., & Migliaccio, M. 2024a, arXiv:2402.13115
Favale, A., Gómez-Valent, A., & Migliaccio, M. 2024b, PhLB, 858, 139027
Gardner, J. P., Mather, J. C., Clampin, M., et al. 2006, SSRv, 123, 485
Gil-Marín, H., Percival, W. J., Verde, L., et al. 2017, MNRAS, 465, 1757
Gómez-Valent, A., Favale, A., Migliaccio, M., & Sen, A. A. 2024, PhRvD, 109, 023525
Gómez-Valent, A., Mavromatos, N. E., & Solà Peracaula, J. 2023, CQGra, 41, 015026
Gómez-Valent, A., & Solà Peracaula, J. 2018, MNRAS, 478, 126
Grande, J., Pelinson, A., & Solà, J. 2009, PhRvD, 79, 043006
Grande, J., Solà, J., & Stefancic, H. 2006, JCAP, 08, 011
Grande, J., Solà, J., & Stefancic, H. 2007, PhLB, 645, 236
Guzzo, L., Pierleoni, M., Meneux, B., et al. 2008, Natur, 451, 541
Hastings, W. K. 1970, Bimka, 57, 97
Heinesen, A., Blake, C., & Wiltshire, D. L. 2020, JCAP, 01, 038
Heisenberg, L., Villarrubia-Rojo, H., & Zosso, J. 2022, PhRvD, 106, 043503
Hou, J., Sánchez, A. G., Ross, A. J., et al. 2020, MNRAS, 500, 1201
Jiménez, R., Verde, L., Treu, T., & Stern, D. 2003, ApJ, 593, 622

Labbé, I., van Dokkum, P., Nelson, E., et al. 2023, Natur, 616, 266
Lesgourgues, J. 2011, arXiv:1104.2932
Lewis, A. 2019, arXiv:1910.13970
Marra, V., & Perivolaropoulos, L. 2021, PhRvD, 104, L021303
Mavromatos, N. E. 2022, RSPTA, 380, 20210188
Mavromatos, N. E., Dorlis, P., & Vlachos, S.-N. 2024, arXiv:2404.18741
Mavromatos, N. E., & Solà Peracaula, J. 2021a, EPJP, 136, 1152
Mavromatos, N. E., & Solà Peracaula, J. 2021b, EPJST, 230, 2077
Menci, N., Adil, S. A., Mukhopadhyay, U., Sen, A. A., & Vagnozzi, S. 2024, JCAP, 07, 072
Metropolis, N., Rosenbluth, A. W., Rosenbluth, M. N., Teller, A. H., & Teller, E. 1953, JChPh, 21, 1087
Mohammad, F. G., Bianchi, D., Percival, W. J., et al. 2018, A&A, 619, A17
Moreno-Pulido, C., & Solà, J. 2020, EPJC, 80, 692
Moreno-Pulido, C., & Solà Peracaula, J. 2022a, EPJC, 82, 551
Moreno-Pulido, C., & Solà Peracaula, J. 2022b, EPJC, 82, 1137
Moreno-Pulido, C., Solà Peracaula, J., & Cheraghchi, S. 2023, EPJC, 83, 637
Moresco, M. 2015, MNRAS, 450, L16
Moresco, M., Cimatti, A., Jimenez, R., et al. 2012, JCAP, 1208, 006
Moresco, M., Jimenez, R., Verde, L., Cimatti, A., & Pozzetti, L. 2020, ApJ, 898, 82
Moresco, M., Pozzetti, L., Cimatti, A., et al. 2016, JCAP, 1605, 014
Okumura, T., Hikage, C., Totani, T., et al. 2016, PASJ, 68, 38
Orchard, L., & Cárdenas, V. H. 2024, PDU, 46, 101678
Padmanabhan, T. 2003, PhR, 380, 235
Pan, J., Huterer, D., Andrade-Oliveira, F., & Avestruz, C. 2024, JCAP, 06, 051
Peebles, P. J. E. 1993, Principles of Physical Cosmology (Princeton, NJ: Princeton Univ. Press)
Peebles, P. J. E., & Ratra, B. 2003, RvMP, 75, 559
Perivolaropoulos, L., & Skara, F. 2021, PhRvD, 104, 123511
Perivolaropoulos, L., & Skara, F. 2022a, NewAR, 95, 101659
Perivolaropoulos, L., & Skara, F. 2022b, Univ, 8, 502
Ratsimbazafy, A. L., Loubser, S. I., Crawford, S. M., et al. 2017, MNRAS, 467, 3239
Riess, A. G., Yuan, W., Macri, L. M., et al. 2022, ApJL, 934, L7
Rubin, D., Aldering, G., Betoule, M., et al. 2023, arXiv:2311.12098
Said, K., Colless, M., Magoulas, C., Lucey, J. R., & Hudson, M. J. 2020, MNRAS, 497, 1275
Sanchez, A. G. 2020, PhRvD, 102, 123511
Semenaite, A., Sanchez, A. G., Pezzotta, A., et al. 2022, MNRAS, 512, 5657
Semenaite, A., Sanchez, A. G., Pezzotta, A., et al. 2023, MNRAS, 521, 5013
Simon, J., Verde, L., & Jiménez, R. 2005, PhRvD, 71, 123001
Simpson, F., Blake, C., Peacock, J. A., et al. 2016, PhRvD, 93, 023525
Solà, J. 2013, JPhCS, 453, 012015
Solà, J., & Gómez-Valent, A. 2015, IJMPD, 24, 1541003
Solà, J., Gómez-Valent, A., & de Cruz Pérez, J. 2015, ApJL, 811, L14
Solà, J., Gómez-Valent, A., & de Cruz Pèrez, J. 2017, ApJ, 836, 43
Solà Peracaula, J. 2022, RSPTA, 380, 20210182
Solà Peracaula, J., de Cruz Pérez, J., & Gómez-Valent, A. 2018a, EPL, 121, 39001
Solà Peracaula, J., de Cruz Pérez, J., & Gómez-Valent, A. 2018b, MNRAS, 478, 4357
Solà Peracaula, J., Gómez-Valent, A., & de Cruz Pérez, J. 2017, PhLB, 774, 317
Solà Peracaula, J., Gómez-Valent, A., & de Cruz Pérez, J. 2019, PDU, 25, 100311
Solà Peracaula, J., Gómez-Valent, A., de Cruz Pérez, J., & Moreno-Pulido, C. 2021, EPL, 134, 19001
Solà Peracaula, J., Gómez-Valent, A., de Cruz Pérez, J., & Moreno-Pulido, C. 2023, Univ, 9, 262
Song, Y.-S., & Percival, W. J. 2009, JCAP, 0910, 004
Spiegelhalter, D. J., Best, N. G., Carlin, B. P., & Van Der Linde, A. 2002, J. Roy. Stat. Soc., 64, 583
Stern, D., Jimenez, R., Verde, L., Kamionkowski, M., & Stanford, S. A. 2010, JCAP, 1002, 008
Tomasetti, E., Moresco, M., Borghi, N., et al. 2023, A&A, 679, A96
Turner, M. S. 2022, ARNPS, 72, 1
Weinberg, S. 1989, RvMP, 61, 1
Zhang, C., Zhang, H., Yuan, S., et al. 2014, RAA, 14, 1221
Zhao, G.-B., Raveri, M., Pogosian, L., et al. 2017, NatAs, 1, 627